TRAMPOLINE Si_3N_4 MAGNETOMETERS WITH 330 PT/$\sqrt{Hz}$ SENSITIVITY

Massood Tabib-Azar and Brian Baker
University of Utah, Salt Lake City, Utah, USA

ABSTRACT

We discuss and report a magnetometer using a sensor structure consisting of two parallel silicon nitride trampoline membranes functionalized with yttrium iron garnet (YIG) with 330 pT/$\sqrt{Hz}$ sensitivity for the first time. Trampoline sensors are shown to have a very low force noise density approaching ~ 10^{-18} $N/\sqrt{Hz}$ and very high-quality factor resonant modes can be separately tracked to compensate for temperature drifts and environmental interferences or to sense multiple measurands simultaneously. Functionalization of the trampoline membrane with ferrimagnetic and non-linear optical materials along with light squeezing using the same membrane leads to improved displacement sensing.

KEYWORDS

Optomechanics, Ultrasensitive Sensor Platform, High-Q Resonators, Quantum Sensors

INTRODUCTION

High tensile stress silicon nitride trampoline membranes [1] are excellent candidates for ultrasensitive devices to detect displacement, acceleration, force, and temperature as primary measurands. Through functionalization, trampoline sensors are also reported for other entities such as chemical and biochemical agents, biomarkers, gases, radiation, etc. For example, they have been used in detecting mid-IR signals with 7 pW/$\sqrt{Hz}$ sensitivity [2-4], as spin transition sensors in negatively charged nitrogen vacancies in diamond sensors [5], electric field [6], position [7], general [8], methane [9], and microbalance [10]. Many different trampoline excitation/sensing techniques including optomechanical, piezoelectric, electrostatic, and magnetomotive methods are developed and reported [1-8]. A combination of very small mass and high tensile stress in Si_3N_4 trampoline structures results in multimodal resonances in the 50-200 kHz range. Here for the first time, we report the design and fabrication of two aligned and parallel Si_3N_4 trampoline structures on the opposite sides of a silicon wafer. We next demonstrated their application in magnetometry by using a yttrium iron garnet (YIG) particle [11] attached to their central platform region with the resulting sensitivity of 330 pT/$\sqrt{Hz}$.

Sensor Design and Operation Principles: The trampoline structure is composed of 4 stretched nitride beams connecting the corners of a silicon frame to a central nitride pad (Figs. 1 and 2). The nitride layer can be as thin as a few nanometers and the beams can be as narrow as ~1 µm. Unlike mass loading or temperature increase that usually downshift the resonance frequency (f_r), low frequency (f_m<f_r) magnetic flux densities upshift the trampoline resonance frequency by (incrementally) increasing its tension (Fig. 1b). One can also take advantage of the torque generated by the external field on the YIG when it is magnetized to excite asymmetrical modes twisting mode is shown in Fig. 1c.

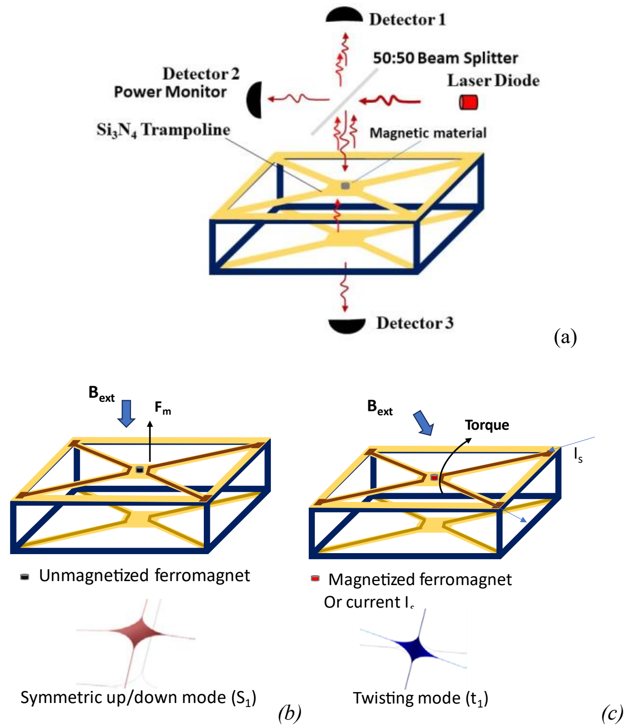

Fig. 1. a) Schematic of the trampoline sensor structure. A small particle of yttrium iron garnet (YIG) was used on the top trampoline. The two parallel trampolines can be used as an interferometer. b) The external flux density applies a force on the trampoline with YIG and alters its s_1 resonance. c) If the YIG is magnetized, the external flux density applies a torque and can cause the excitation of the twisting (t_1) vibration mode.

Device Fabrication: The steps used in the fabrication of the trampoline devices are given in [1]. The low-pressure chemical vapor deposited near-stoichiometric silicon nitride tensile stress was ~861.3 MPa measured using Tencor Flexus (wafer bowing technique). We used CF_4/O_2 reactive ion etching with a 90 nm/min nitride etch rate. Fig. 2 shows images of the trampoline sensor. Dimensions of different parts of the sensor are shown in Figs. 2a and 2b. 55 ^{0}C KOH bath was used to etch through the silicon wafer from both sides resulting in 3x3 mm^2 opening (Fig. 2c). The two trampoline structures on the same sensor are shown in Fig. 2d. We attached YIG particles (~10-100 µm diameter) by first putting a very small droplet of superglue on the trampoline platform and then by sprinkling YIG powder over it. We then used a gentle nitrogen flow to remove the YIG particles everywhere except on the platform where they were glued.

978-1-940470-05-4/HH2024/$25©2024TRF
DOI 10.31438/TRF.HH2024.59

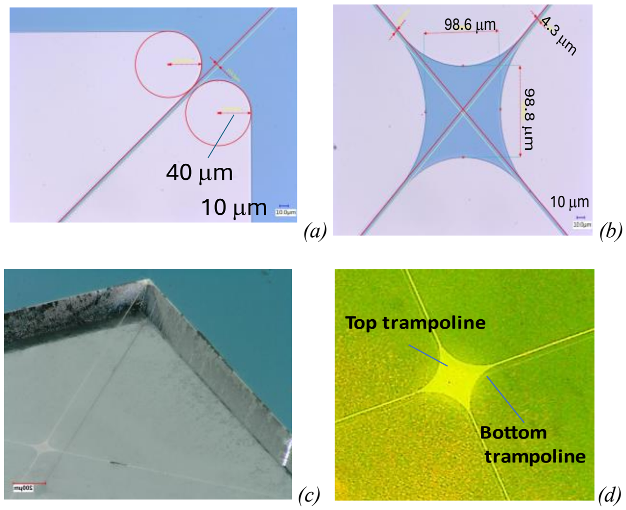

Fig. 2. Optical images of a) rounded corner structure, b) trampoline, c) silicon etch through, and d) top and bottom trampolines.

The initial yield of fabrication was very close to 85%. The trampoline structures are very fragile and should be handled very carefully to prevent damage. Once they were fixed on the laser anemometer stage, they were very robust and stable.

Experimental Procedures and Results

Chips containing 4 trampoline devices were fixed on a piezoelectric resonator disk schematically shown in Fig. 3a. with a spacer preventing the bottom trampoline from touching the disk's surface. A laser Doppler anemometer along with a 10 Hz-500 MHz network analyzer was then used to measure the top trampoline's vibrations spectra.

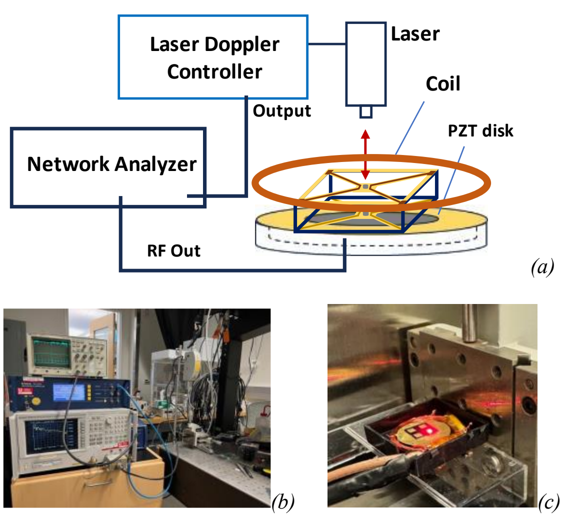

Fig. 3. a) Schematic of the experimental set up. The coil is used to apply the magnetic flux density. b) Image of the setup and c) closeup image of the sample holder stage.

The experimental setup also included a micrometer stage (Figs. 3b and 3c) that enabled the positioning of the trampoline under the laser doppler anemometer for precise alignment and optimum transduction. A coil was used under the piezoelectric disk to apply magnetic flux density (B_e) to the trampoline sample that was functionalized with a YIG particle for magnetometry. Trampoline sensors with YIG particles could be magnetically and acoustically excited with the coil and with the piezoelectric disk, respectively.

The vibration spectra of the silicon frame and the silicon nitride trampoline obtained using the piezoelectric disk excitation are shown in Fig. 4. The trampoline structure has many resonances corresponding to its different excitation modes (Fig. 1).

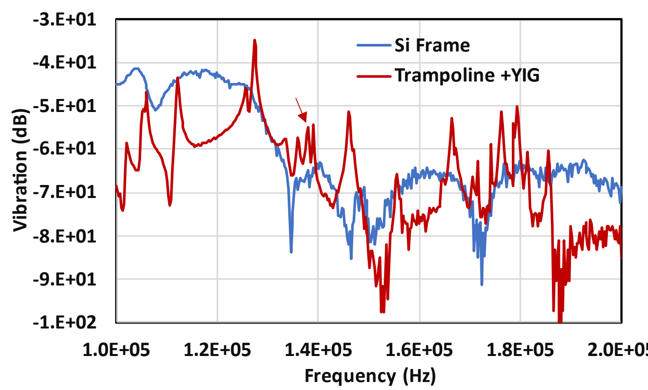

Fig. 4. Vibration spectra of the trampoline sensor. The resonance peak shown with the red arrow is at 138 kHz used in magnetometry.

The effect of the magnetic field on the trampoline vibration amplitude was measured at 138 kHz. The B_e was generated by passing a current through the coil that was situated under the piezoelectric disk (Fig. 3c). The magnitude of the current for generating a specific B_e was calibrated using a Nano-Tesla meter. The piezoelectric disk was used to acoustically excite the trampoline at 138 kHz.

Fig. 5a shows the output of the laser Doppler anemometer as a function of B_e. At 0 nT, the amplitude is maximum. As the B_e increased from zero, the trampoline resonance shifted to higher frequencies and the trampoline vibration magnitude decreased.

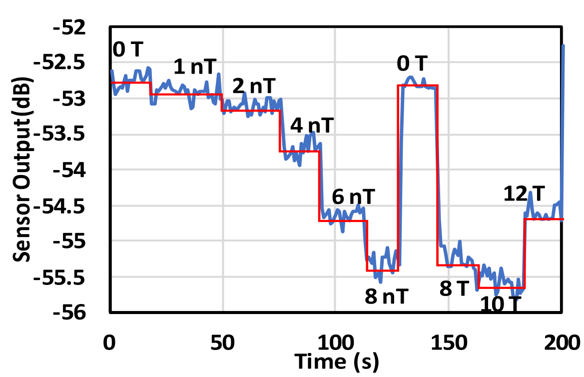

(a)

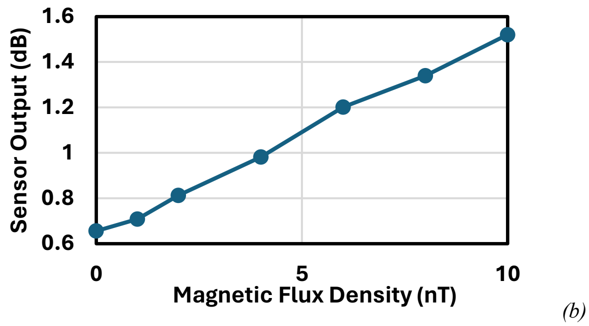

Fig. 5: a) Sensor output at 138 kHz (shown by the red arrow in Fig. 4) as a function of time as the external magnetic flux changed from 0 T up to 12 nT obtained with 10 Hz bandwidth. The resulting Minimum Detectable signal was 330 pT/$\sqrt{Hz}$. b) Sensor output as a function of the external magnetic flux constructed from (a).

Fig. 5b shows the change in the sensor output as a function of B_e. The sensor sensitivity calculated from the slope of this curve is 2.5 mV/nT or 2.5x10^6 V/T.

Fig. 6 shows the spectra of an infrared laser before and after frequency doubling by passing it through a potassium titanyl phosphate (KTP) crystal. The green laser linewidth was ~ 4 nm while that of the infrared laser was 65 nm. Measuring the trampoline sensitivity using the green laser and a Fabry-Perot setup resulted in doubling its sensitivity to 5 mV/nT.

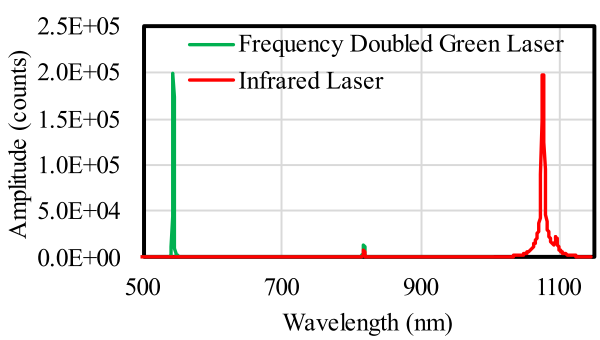

Fig. 6: Spectra of an infrared laser and after its frequency doubling using a non-linear crystal.

We are in the process of using the parallel trampoline structure with appropriate functionalization itself as a Fabry-Perot resonator structure [12] to improve its field sensitivity further.

ACKNOWLEDGEMENTS

This work is partially supported by the USTAR program.

REFERENCES:

1. Reinhardt, C., Muller, T., Bourassa, A., & Sankey, J. C. (2016). Ultralow-noise SiN trampoline resonators for sensing and optomechanics. Physical Review X, 6(2), 021001 (021008 pp.). doi:10.1103/PhysRevX.6.021001
2. Liu, Y., Watkins, C. A., & Feng, P. X. L. (2023). Analysis of Thermal Infrared Detection via Silicon Nitride Trampoline Nanomechanical Resonator 2023 IEEE Research and Applications of Photonics in Defense Conference (RAPID), 2023, Piscataway, NJ, USA.
3. Vicarelli, L., Tredicucci, A., & Pitanti, A. (2022). Micromechanical Bolometers for Subterahertz Detection at Room Temperature. ACS Photonics, 9(2), 360-367. doi:10.1021/acsphotonics.1c01273
4. Piller, M., Hiesberger, J., Wistrela, E., Martini, P., Luhmann, N., & Schmid, S. (2023). Thermal IR Detection With Nanoelectromechanical Silicon Nitride Trampoline Resonators. IEEE Sensors Journal, 1066-1071. doi:10.1109/JSEN.2022.3223439
5. Fischer, R., McNally, D. P., Reetz, C., Assumpcao, G. G. T., Knief, T., Lin, Y., & Regal, C. A. (2019). Spin detection with a micromechanical trampoline: towards magnetic resonance microscopy harnessing cavity optomechanics. New Journal of Physics, 21(4), 043049 (043013 pp.). doi:10.1088/1367-2630/ab117a
6. Z. Han, F. Xue, J. Hu and J. He, "Trampoline-Shaped Micro Electric-Field Sensor for AC/DC High Electric Field Measurement," in *IEEE Transactions on Industrial Electronics*, vol. 69, no. 12, pp. 13791-13798, Dec. 2022, doi: 10.1109/TIE.2021.3131880.
7. Miao-Hsuan Chien, Johannes Steurer, Pedram Sadeghi, Nicolas Cazier, and Silvan Schmid, "Nanoelectromechanical Position-Sensitive Detector with Picometer Resolution," CS Photonics 2020, 7, 8, 2197–2203.
8. Dantan, A. (2020). Nanostructured trampoline microcavities for sensing and optomechanics. Paper presented at the High Contrast Metastructures IX, 3-6 Feb. 2020, USA.
9. Zenghui, W., Peng, W., Jaesung, L., Chung-Chiun, L., & Feng, P. X. L. (2015). Towards real-time methane (CH4) capture and detection by nanoparticle-enhanced silicon carbide trampoline oscillators. Paper presented at the 2015 Transducers - 18th International Conference on Solid-State Sensors, Actuators and Microsystems (TRANSDUCERS), 21-25 June 2015, Piscataway, NJ, USA.
10. Luhmann, N., Pliessnig, R., Lafleur, J. P., & Schmid, S. (2021). Quantitative analysis by nanoelectromechanical photothermal infrared spectroscopy with picogram sensitivity. 2021 Conference on Lasers and Electro-Optics (CLEO), 9-14 May 2021, Piscataway, NJ, USA.
11. Tabib-Azar, M., Lam, O.T. (2023), Yttrium Iron Garnet Magnetometers with 10 nT/SQRT(Hz) Sensitivity. IEEE Sensors, Vienna Austria, (10/30-11/4)
12. Aggarwal, N., Cullen, T. J., Cripe, J., Cole, G. D., Lanza, R., Libson, A., . . . Mavalvala, N. (2020). Room-temperature optomechanical squeezing. Nature Physics, 16(7), 784-788. doi:10.1038/s41567-020-0877-x

CONTACT

*Massood Tabib-Azar, tel: +1-216-534-7670; azar.m@utah.edu